J. Am. Chem. Soc. **1987**, *109*, 3428–3436

Kinetics and Mechanism of Oxygen Transfer in the Reaction of *p*-Cyano-*N*,*N*-dimethylaniline *N*-Oxide with Metalloporphyrin Salts. 5. The Influence of Imidazole Ligation of (*meso*-Tetrakis(2,6-dimethylphenyl)porphinato)manganese(III) Chloride on the Rates of Oxygen Transfer from *N*-Oxide to Metalloporphyrin Salt and the Efficiency of Oxidations by the Intermediate Higher Valent Manganese–Oxo Species

Wah-Hun Wong, Dražen Ostović, and Thomas C. Bruice*

Contribution from the Department of Chemistry, University of California, Santa Barbara, California 93106. *Received September 12, 1986*

Abstract: Equilibrium constants for mono- and bisligation of imidazole (ImH) with (*meso*-tetrakis(2,6-dimethylphenyl)-porphinato)manganese(III) chloride ($(Me_8TPP)Mn^{III}Cl$) have been determined so that the concentrations (dry CH_2Cl_2) of the three species $(Me_8TPP)Mn^{III}Cl$, $[(Me_8TPP)Mn^{III}(ImH)]Cl$, and $[(Me_8TPP)Mn^{III}(ImH)_2]Cl$ may be calculated at different ImH concentrations. The equilibrium constants for ligation of the one and two imidazoles are $K_1 = 245\ M^{-1}$ and $\beta_2 = 1.80 \times 10^5\ M^{-2}$. The reaction of *p*-cyano-*N*,*N*-dimethylaniline *N*-oxide (NO) with the manganese(III) porphyrin (under the pseudo-first-order conditions of $[NO]_i \gg [(Me_8TPP)Mn^{III}Cl]_i$ and in the presence and absence of ImH) is first order in both NO and manganese(III) porphyrin, and the rate-controlling step involves oxygen transfer with formation of higher valent manganese–oxo porphyrin species plus *p*-cyano-*N*,*N*-dimethylaniline (DA). From the dependence of the pseudo-first-order rate constants (k_{obsd}) upon $[ImH]_i$ and a knowledge of the equilibrium constants for imidazole ligation there has been calculated the second-order rate constants for the kinetic terms $k_1[NO][(Me_8TPP)Mn^{III}Cl]$, $k_2[NO][[(Me_8TPP)Mn^{III}(ImH)]Cl]$, and $k_3[NO][[(Me_8TPP)Mn^{III}(ImH)_2]Cl]$. Comparison of the second-order rate constants ($k_1 = 3.3 \times 10^{-2}\ M^{-1}\ s^{-1}$, $k_2 = 5.53\ M^{-1}\ s^{-1}$, and $k_3 = 7.32 \times 10^{-2}\ M^{-1}\ s^{-1}$) establishes that ligation by one imidazole increases the rate of reaction of the manganese(III) porphyrin with NO by ~166-fold. Bis-imidazole ligated species are blocked to reaction with NO. The higher valent manganese–oxo porphyrin species formed from the reaction of NO with $[(Me_8TPP)Mn^{III}(ImH)]Cl$ has been shown to be the principal epoxidizing agent from the dependence of the percentage yield of epoxide upon the concentration of ImH in reactions with *cis*-cyclooctene using constant initial concentrations of $(Me_8TPP)Mn^{III}Cl$ and NO. Epoxidation reactions are not rate controlling, and epoxide is formed in competitive processes that involve the reaction of higher valent manganese–oxo porphyrin species with DA (and its oxidation products) and alkene. With the exception of the sterically hindered *trans*-β-methylstyrene, the percentage yield of epoxide at 1.0 M alkene is essentially independent of the type of alkene. Increase in the concentration of alkene and the $1e^-$ oxidizable 2,4,6-tri-*tert*-butylphenol fails to trap all higher valent manganese–oxo porphyrin species. This result is interpreted as being due to the initial formation of an intimate pair of oxo species and DA with competition between dissociation of DA and oxo species and oxidation of DA within the intimate pair. Epoxidation of alkene by the oxo species occurs after the latter dissociates from the intimate pair.

p-Cyano-*N*,*N*-dimethylaniline *N*-oxide (NO) has been proven to be a particularly useful oxygen atom donor to iron(III) and manganese(III) porphyrins.[1,2] In an earlier study[1] we investigated the influence of the nature of the axial ligand (X^- = F^-, Cl^-, Br^-, I^-, OCN^-) on the kinetics of the reaction of (*meso*-tetraphenylporphinato)manganese(III) (i.e., $(TPP)Mn^{III}X$) with NO in the presence of alkene (eq 1, where DA represents *p*-cyano-*N*,*N*-dimethylaniline and MA represents *p*-cyano-*N*-methylaniline).

$$(TPP)Mn^{III}X + NO \underset{k_{-1}}{\overset{k_1}{\rightleftharpoons}} (TPP)Mn^{III}(X)(NO) \quad (1a)$$

$$(TPP)Mn^{III}(X)(NO) \xrightarrow{k_2} [[(TPP)(X)(MnO)]\cdots DA] \quad (1b)$$

$$[[(TPP)(X)(MnO)]\cdots DA] \xrightarrow{k_3} (TPP)Mn^{III}X + MA + CH_2O \quad (1c)$$

$$[[(TPP)(X)(MnO)]\cdots DA] \xrightarrow{k_4} [(TPP)(X)(MnO)] + DA \quad (1d)$$

$$[(TPP)(X)(MnO)] + \text{alkene} \xrightarrow{k_5} (TPP)Mn^{III}X + \text{epoxide} \quad (1e)$$

From computer simulation of the time courses for the formation of MA and epoxide it was concluded that: (i) oxygen transfer from NO occurs through the reversible formation of the hexacoordinated species, $(TPP)Mn^{III}(X)(NO)$, which subsequently decomposes to the intimate pair $[[(TPP)(X)(MnO)]\cdots DA]$; (ii) the intimate pair undergoes the competing reactions of internal oxidation of DA (eq 1c) and diffusion apart (eq 1d); and (iii) all epoxide formation occurs by reaction of alkene with [(TPP)-(X)(MnO)] (eq 1e) after the latter's diffusion from association with DA. The rates of product formation were shown to be dependent upon the nature of the axial ligand X^-. The pseudo-first-order rate constants for turnover, when X^- = Cl^-, Br^-, I^-, and OCN^-, were found to have a first-order dependence on $[(TPP)Mn^{III}X]$ and to be independent of the concentration of NO. When X^- is F^-, however, $(TPP)Mn^{III}F$ catalyst was found to be saturated with NO so that the appearance of products was zero order. In comparing the rate and equilibrium constants for the reaction of $(TPP)Mn^{III}F$ and $(TPP)Mn^{III}Cl$ it was found that the

(1) Powell, M. F.; Pai, E. F.; Bruice, T. C. *J. Am. Chem. Soc.* **1984**, *106*, 3277.

(2) (a) Shannon, P.; Bruice, T. C. *J. Am. Chem. Soc.* **1981**, *103*, 4500. (b) Nee, M. W.; Bruice, T. C. *Ibid.* **1982**, *104*, 6123. (c) Dicken, C. M.; Lu, F.-L.; Nee, M. W.; Bruice, T. C. *Ibid.* **1985**, *107*, 5776. (d) Dicken, C. M.; Woon, T. C.; Bruice, T. C. *Ibid.* **1986**, *108*, 1636. (e) Woon, T.-C.; Dicken, C. M.; Bruice, T. C. *J. Am. Chem. Soc.* **1986**, *108*, 7990.

0002-7863/87/1509-3428$01.50/0

equilibrium constant for the formation of (TPP)Mn(X)(NO) species is approximately 700 times larger when $X^- = F^-$ (eq 1a), whereas the rate constant for demethylation (eq 1c) is approximately 70 times smaller. Thus, the nature of the axial ligand may have a profound influence upon the overall rate and kinetic behavior in the formation of the higher valent manganese–oxo porphyrin species and also on the rate constants for the reaction of this species with substrates.

The nature of the axial ligand also has a profound influence on the reactivity of manganese(III) porphyrin salts with other oxygen atom donors. Manganese(III) porphyrin salts are good catalysts for oxidations with iodosylbenzene and percarboxylic acids but are unreactive toward alkyl hydroperoxides.[3] However, reactions of alkyl hydroperoxides as well as hypochlorite, another single oxygen donor, have been shown to be greatly enhanced by ligation of the Mn(III) porphyrin with heterocyclic bases including imidazole[4,5] and pyridines.[6] Apparently, alteration of the spin state of $(TPP)Mn^{III}Cl$ from high spin to low spin by replacement of the weaker axial ligand (Cl^-) by a stronger field ligand (N-base)[7] causes rate enhancement and is also reported to influence the catalyst stability and product stereochemistry.[6a,c] Typically, Meunier[6b] and Mansuy[5c] have shown that pyridine and imidazole ligation of $(TPP)Mn^{III}Cl$ results in an increase in the stereoselectivity and yield of epoxidation of *cis*-stilbene when using NaOCl and cumyl hydroperoxide as oxygen-transfer agents. Collman[5a,b] has also taken advantage of nitrogen base ligation in his investigations of epoxidation of alkenes by hypochlorite. In a recent quantitative study of the kinetics of oxygen atom transfer from percarboxylic acids and alkyl hydroperoxides (YOOH) to manganese(III) tetraphenylporphyrin, it was shown that a linear free-energy relationship exists between the log of the second-order rate constants vs. the pK_a of the leaving groups (YOH) (eq 2).

$$\log k_{YOOH} = \beta_{lg} pK_a(YOH) + C \qquad (2)$$

Exchange of Cl^- ligand for imidazole decreases the slope of the plot of log k_{YOOH} vs. pK_a from $\beta_{lg} = -1.3$ to -0.7 and increases the value of C by $\sim 10^4$. Due to these changes the rate of oxygen transfer to Mn(III) porphyrin from both percarboxylic acids and alkyl hydroperoxides is greatly accelerated.[4a] The acceleration of rate is truly remarkable for the weakly acidic alkyl hydroperoxides.

There is described herein a detailed study of the influence of imidazole upon the reaction of NO with (*meso*-tetrakis(2,6-dimethylphenyl)porphinato)manganese(III) chloride ($(Me_8TPP)Mn^{III}Cl$). Epoxidation reactions of a variety of alkenes have also been investigated. The porphyrin ligand, *meso*-tetrakis(2,6-dimethylphenyl)porphyrin, is used to obviate complications due to μ-oxo dimer formation and also because the system NO + $(Me_8TPP)Fe^{III}Cl$ provides yields of epoxides which exceed 80% based upon initial concentrations of NO.[2e]

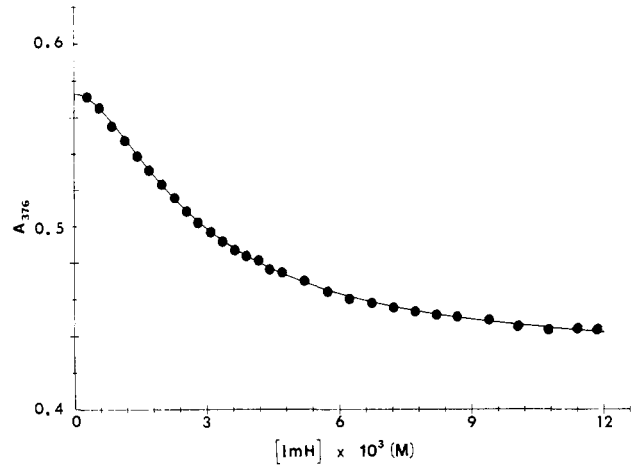

Figure 1. Representative plot of A_{376} vs. [ImH] used for the determination of K_1 and β_2. $[(Me_8TPP)Mn^{III}Cl]_0 = 1.19 \times 10^{-5}$ M ($\epsilon_0 = 4.80 \times 10^4$ M^{-1} cm^{-1}) and [ImH] was varied between 2.9×10^{-4} and 1.19×10^{-2} M. The points are experimentally determined, and the line was drawn by using eq 7 and computer-fitted constants: $K_1 = (2.53 \pm 0.53) \times 10^2$ M^{-1}, $\beta_2 = (1.94 \pm 0.24) \times 10^5$ M^{-2}, $\epsilon_1 = (4.83 \pm 0.09) \times 10^4$ M^{-1} cm^{-1}, and $\epsilon_2 = (3.55 \pm 0.02) \times 10^4$ M^{-1} cm^{-1}.

Experimental Section

Absorption spectra were recorded on a Cary 118C. Spectral kinetic data were recorded with a Perkin-Elmer 553 fast-scanning UV–vis spectrophotometer equipped with a constant-temperature multicell holder maintained at 25 ± 0.2 °C. GC analyses were carried out with a Varian Model 3700 gas chromatograph coupled to a Hewlett-Packard 3392A integrator. A 20-m capillary column (Varian, WCOT, Vit. Silica) was used. HPLC analyses were performed on a system consisting of a two Altex dual-stroke pumps, Altex solvent programmer, Altex RSIL CN analytical column (5 μm, 250 × 4.6 mm), an HP1040A diode-array UV detector, and two HP3392A integrators. Pseudo-first-order rate constants were determined from plots of kinetic data by use of a Hewlett-Packard 9825A computer equipped with 9864A digitizer and 9862A plotter.

Materials. Dichloromethane was purified in the manner previously described.[2c] *p*-Cyano-*N*,*N*-dimethylaniline *N*-oxide (NO) was prepared in a manner previously reported.[2c] Alkenes of the highest purity were purchased from Aldrich and further purified in the following manner: 2,3-dimethyl-2-butene (TME) was distilled in a dry N_2 glove box over P_2O_5 through a Vigreux column and then passed through activated basic alumina followed by passing through an activated neutral alumina column just before use; *cis*-cyclooctene, cyclohexene, cyclopentene, and *trans*-β-methylstyrene were distilled in a dry N_2 glove box from powdered fused NaOH through a Vigreux column and the passed through activated neutral alumina before use; norbornylene was sublimed before use. 2,4,6-Tri-*tert*-butylphenol (TBPH) from Aldrich was recrystallized from $EtOH/H_2O$ (3 times) and then sublimed. Imidazole (ImH) from Aldrich was twice recrystallized from benzene and vacuum dried. *meso*-Tetrakis(2,6-dimethylphenyl)porphyrin $(Me_8TPP)H_2$ was synthesized by the method of Zipplies, Lee, and Bruice.[8] (*meso*-Tetrakis(2,6-dimethylphenyl)porphinato)manganese(III) chloride ($(Me_8TPP)Mn^{III}Cl$) was prepared from $(Me_8TPP)H_2$ by using a modified procedure of Adler[9] and purified by repeated column chromatography over neutral alumina ($CHCl_3$ as eluant): UV–vis (λ_{max}, nm; ϵ, M^{-1} cm^{-1}) 372 (5.08×10^4), 398 (3.98×10^4), 478 (1.13×10^5), 585 (9.8×10^3), 620 (1.10×10^4); mass spectrum, m/z 815 $(M)^+$, 780 $(M - Cl)^+$. Authentic epoxides were used to generate standard plots for GC analyses: TME oxide (TMEO) was synthesized by a standard procedure[10] from TME and *m*-chloroperbenzoic acid in CH_2Cl_2 and purified by distillation. All other epoxides were purchased from Aldrich. *p*-Cyano-*N*,*N*-dimethylaniline (DA), *p*-cyano-*N*-methylaniline (MA), *N*,*N*′-dimethyl-*N*,*N*′-bis(*p*-cyanophenyl)hydrazine (H), *N*,*N*′-bis(*p*-cyanophenyl)-*N*-methylmethylenediamine (MD), *p*-cyanoaniline (A), and *N*-formyl-*p*-cyano-*N*-methylaniline (FA) used for HPLC calibration were obtained as described in an earlier paper.[2c]

(3) (a) Yuan, L.-C.; Bruice, T. C. *Inorg. Chem.* **1985**, *24*, 986. (b) Mansuy, D.; Bartoli, J. F.; Momenteau, M. *Tetrahedron Lett.* **1982**, *23*, 2781. (c) Mansuy, D.; Bartoli, J. F.; Chottard, J.-C.; Lange, M. *Angew. Chem., Int. Ed. Engl.* **1980**, *19*, 909. (d) Hill, C. L.; Smegal, J. A.; Henly, T. J. *J. Org. Chem.* **1983**, *48*, 3277.

(4) (a) Yuan, L.-C.; Bruice, T. C. *J. Am. Chem. Soc.* **1986**, *108*, 1643. (b) Balasubramanian, P. N.; Sinha, A.; Bruice, T. C. *J. Am. Chem. Soc.* **1987**, *109*, 1456.

(5) (a) Collman, J. P.; Brauman, J. I.; Meunier, B.; Hayashi, T.; Kodadek, T.; Raybuck, S. A. *J. Am. Chem. Soc.* **1985**, *107*, 2000. (b) Collman, J. P.; Brauman, J. I.; Meunier, B.; Raybuck, S. A.; Kodadek, T. *Proc. Natl. Acad. Sci. U.S.A.* **1984**, *81*, 3245. (c) Mansuy, D.; Battioni, P.; Renaud, J.-P. *J. Chem. Soc., Chem. Commun.* **1984**, 1255.

(6) (a) Guilmet, E.; Meunier, B. *Nouv. J. Chim.* **1982**, *6*, 511. (b) Meunier, B.; Guilmet, E.; Carvalho, M.-E.D.; Poilblanc, R. *J. Am. Chem. Soc.* **1984**, *106*, 6668. (c) Collman, J. P.; Kodadek, T.; Raybuck, S. A.; Meunier, B. *Proc. Natl. Acad. Sci. U.S.A.* **1983**, *80*, 7039. (d) Guilmet, E.; Meunier, B. *J. Mol. Catal.* **1984**, *23*, 115. (e) Van der Made, A. W.; Nolte, R. J. M. *J. Mol. Catal.* **1984**, *26*, 333. (f) Razenberg, J. A. S. J.; Nolte, R. J. M.; Drenth, W. *Tetrahedron Lett.* **1984**, *25*, 789.

(7) (a) Hansen, A. P.; Goff, H. M. *Inorg. Chem.* **1984**, *23*, 4519. (b) Landrum, J. T.; Hatano, K.; Scheidt, W. R.; Reed, C. A. *J. Am. Chem. Soc.* **1980**, *102*, 6729.

(8) Zipplies, M. F.; Lee, W. A.; Bruice, T. C. *J. Am. Chem. Soc.* **1986**, *108*, 4433.

(9) Adler, A. D.; Longo, F. R.; Kampas, F.; Kim, J. *J. Inorg. Nucl. Chem.* **1970**, *32*, 2443.

(10) Fieser, L. F.; Fieser, M. In *Reagents for Organic Synthesis*; Wiley: New York, 1967; Vol. 1, p 136.

Scheme I

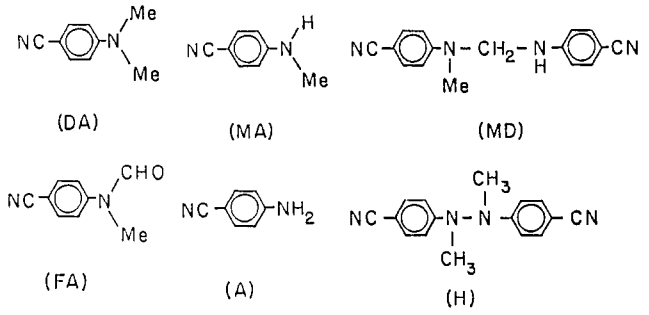

Association constants K_1 and β_2 for binding of imidazole with $(Me_8TPP)Mn^{III}Cl$ were determined by spectroscopic titration. All titrations were done at 25 ± 0.2 °C under N_2 atmosphere. The changes in the spectrum of $(Me_8TPP)Mn^{III}Cl$ upon addition of imidazole were recorded at 30 different concentrations of imidazole ranging from 2.9×10^{-4} to 1.19×10^{-2} M, at $[(Me_8TPP)Mn^{III}Cl] = 1.19 \times 10^{-5}$ M.

Kinetic Method. All reactions have been studied at CH_2Cl_2 solvent at 25 ± 0.2 °C under an anhydrous N_2 atmosphere. The procedures for following the kinetics at 320 or 630 nm (TBP•) and the time course for the formation of DA, MA, H, and MD have been described previously.[2c]

Product Analyses. GC was used to quantitatively determine the various epoxides formed. DA, MA, H, MD, FA, and A formation were analyzed by HPLC. Methods and conditions for GC and HPLC analyses have been described in a previous publication.[2c]

Results

Association constants for ligation of (*meso*-tetrakis(2,6-dimethylphenyl)porphinato)manganese(III) chloride ($(Me_8TPP)Mn^{III}Cl$) by imidazole in methylene chloride at 25 ± 0.2 °C (eq 3–5) were determined by nonlinear least-squares computer fitting[11] of the titration data obtained at eight different wavelengths be-

$$(Me_8TPP)Mn^{III}Cl + ImH \underset{}{\overset{K_1}{\rightleftharpoons}} [(Me_8TPP)Mn^{III}(ImH)]Cl \quad (3)$$

$$[(Me_8TPP)Mn^{III}(ImH)]Cl + ImH \overset{K_2}{\rightleftharpoons} [(Me_8TPP)Mn^{III}(ImH)_2]Cl \quad (4)$$

$$(Me_8TPP)Mn^{III}Cl + 2ImH \overset{\beta_2}{\rightleftharpoons} [(Me_8TPP)Mn^{III}(ImH)_2]Cl \quad (5)$$

$$\beta_2 = K_1K_2 \quad (6)$$

tween 370 and 478 nm to an equation (eq 7) derived by combining eq 3 and 5. In eq 7, A is the absorbance recorded at any given

$$A = [P]_0\left(\frac{\epsilon_0 + \epsilon_1K_1[ImH] + \epsilon_2\beta_2[ImH]^2}{1 + K_1[ImH] + \beta_2[ImH]^2}\right) \quad (7)$$

[ImH], $[P]_0$ equals the concentration of $(Me_8TPP)Mn^{III}$ employed, ϵ_0 is the molar absorbtivity of $(Me_8TPP)Mn^{III}Cl$, and ϵ_1 and ϵ_2 are the molar absorbtivities of $[(Me_8TPP)Mn^{III}(ImH)]Cl$ and $[(Me_8TPP)Mn^{III}(ImH)_2]Cl$, respectively. From the fitting of eq 7 to the titration data (Figure 1) the values of the equilibrium constants were determined to be $K_1 = (2.45 \pm 0.54) \times 10^2$ M^{-1} and $\beta_2 = (1.80 \pm 0.34) \times 10^5$ M^{-2}. Values of ϵ_1 and ϵ_2 are, of course, different for each wavelength employed; as an example see Figure 1.

Dependence of the Kinetics of Decomposition of *p*-Cyano-*N*,*N*-dimethylaniline *N*-Oxide (NO) Catalyzed by $(Me_8TPP)Mn^{III}Cl$. It has been determined, by monitoring spectrophotometrically at 320 nm, that oxygen transfer from NO (6.0×10^{-3} M) to $(Me_8TPP)Mn^{III}Cl$ (4.4×10^{-4} M) in methylene chloride at 25 °C follows the first-order rate law. The reaction is quite slow ($t_{1/2} \sim 13$ h). Dividing the first-order rate constant by

(11) We thank Mr. Vojislav Srdanov for providing the computer program for nonlinear least-squares fitting.

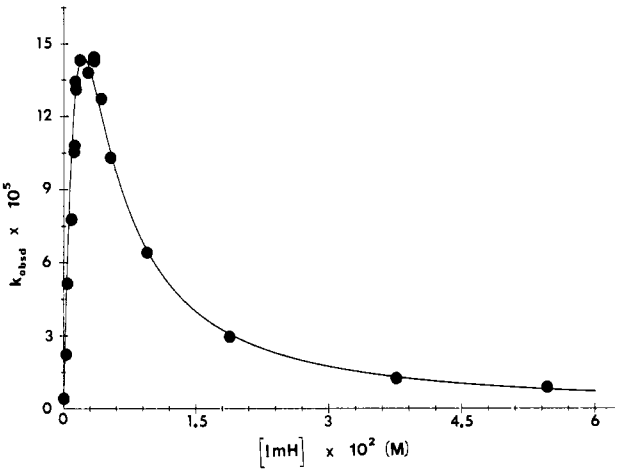

Figure 2. Plot of k_{obsd} vs. imidazole concentration, $[ImH]_i$, for the reaction of NO (2.86×10^{-3} M) with $(Me_8TPP)Mn^{III}Cl$ (1.23×10^{-4} M) at varying $[ImH]_i$. The points are experimental, and the line is a computer fitting of eq 12 employing the constants of Table I.

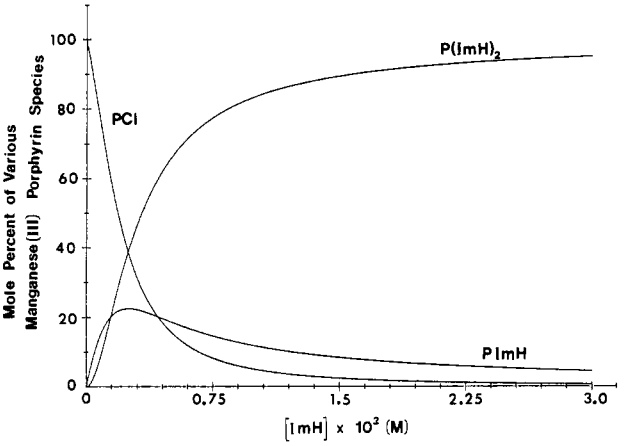

Figure 3. Plots of mole percent of various porphyrin species vs. $[ImH]_i$. For $(Me_8TPP)Mn^{III}Cl$, PCl; for $[(Me_8TPP)Mn^{III}(ImH)]Cl$, PImH; and for $[(Me_8TPP)Mn^{III}(ImH)_2Cl$, $P(ImH)_2$.

Table I. Rate and Equilibrium Constants Employed for the Fitting of the Experimental Points of Figure 2 by Equation 12

constants	values
K_m	30 ± 10 M^{-1}
K_1	245 ± 54 M^{-1}
β_2	$(1.8 \pm 0.34) \times 10^5$ M^{-2}
k_1	$(3.33 \pm 0.17) \times 10^{-2}$ M^{-1} s^{-1}
k_2	5.53 ± 0.33 M^{-1} s^{-1}
k_3	$(7.32 \pm 8.49) \times 10^{-2}$ M^{-1} s^{-1}

$[(Me_8TPP)Mn^{III}Cl]_i$ provides the apparent second-order rate constant, $k_2 = 3.33 \times 10^{-2}$ M^{-1} s^{-1}. HPLC analysis of the reaction mixture at 280 and 320 nm showed complete material balance in both nitrogen and oxygen. The yield of the products DA, MA, MD, A, and CH_2O are 37%, 60%, 2%, 1%, and 30%, respectively, and traces of H and FA were also found (Scheme I).

The influence upon the pseudo-first-order rate constant (k_{obsd}) of the addition of imidazole ($[ImH]_i = 2.3 \times 10^{-4}$ to 5.64×10^{-2} M) when $[(Me_8TPP)Mn^{III}Cl]_i = 1.23 \times 10^{-4}$ M and $[NO]_i = 2.86 \times 10^{-3}$ M (23 turnovers) is shown in Figure 2. Examination of Figure 2 shows that increase in $[ImH]_i$ brings about an initial increase which is then followed by a decrease in the observed rate constant. The maximal rate enhancement occurs at $[ImH]_i \sim 2.2 \times 10^{-3}$ M and amounts to an increase in k_{obsd} of $(1.47 \times 10^{-4}/4.1 \times 10^{-6})$ 36-fold. At high $[ImH]_i$, the pseudo-first-order rate constant approaches very nearly that in the absence of imidazole. Within the concentration range of imidazole used there is present in the kinetic solutions various ratios of the species (Me_8TPP)-

Table II. Effect of $[ImH]_i$ on the Percentage of Products (Based upon $[NO]_i$) and the Material Balance in Oxygen and Nitrogen with $[(Me_8TPP)Mn^{III}Cl]_i = 1.22 \times 10^{-4}$ M and $[NO]_i = 2.87 \times 10^{-3}$ M

	percentage yields							O and N balance, %[a]	
$[ImH]_i$, M	DA	MA	A	H	FA	MD	CH_2O	O	N
0	37	60	1	trace	trace	2	30	99	100
2.32×10^{-4}	44	33	6	3	2	3	23	86	91
4.64×10^{-4}	52	18	6	4	2	4	23	61	86
9.28×10^{-4}	50	13	3	5	1	4	24	39	76
1.16×10^{-3}	46	12	3	6	1	5	29	37	73
1.32×10^{-3}	49	12	2	5	1	4	29	32	73
1.86×10^{-3}	53	5	3	6	2	5	28	32	74
2.78×10^{-3}	51	12	2	7	2	5	28	38	79
3.38×10^{-3}	54	14	4	8	1	10	32	59	91
3.60×10^{-3}	56	23	1	8	1	8	33	59	97
4.18×10^{-3}	57	18	6	6	2	10	34	70	99
5.34×10^{-3}	57	24	1	7	1	8	36	56	98
9.40×10^{-3}	58	37	trace	3	trace	3	39	50	101
1.88×10^{-2}	60	40	0	0	0	0	31	49	100
3.76×10^{-2}	62	39	trace	0	0	0	31	47	101
5.64×10^{-2}	69	32	0	0	0	0	29	35	101

[a] Nitrogen balance, based upon $[NO]_i$, is obtained from the percent yields of DA, MA, A, H, FA, and MD. The percentage oxygen balance, based upon $[NO]_i$, is % O used in the formation of MA, A, H, FA, and MD and the oxidation of CH_2O to HCO_2H. Calculations are carried out as follows: % O used in oxidative formation of nitrogen-containing products = % MA + (2 × % A) + (2 × % FA) + ($^3/_2$ × % H) + ($^3/_2$ × % MD). The % CH_2O which must arise during the reactions = % MA + (2 × % A) + % H + % MD. The % O used to oxidize CH_2O to HCO_2H = (% CH_2O which must arise by dealkylation) − (% CH_2O by Nash assay).

Table III. Effect of $[NO]_i$ on the Pseudo-First-Order Rate Constants (k_{obsd}) with $[(Me_8TPP)Mn^{III}Cl]_i = 1.23 \times 10^{-4}$ M and $[ImH]_i = 1.15 \times 10^{-3}$ M

$[NO]_i$, M	k_{obsd}, s^{-1}	$[NO]_i$, M	k_{obsd}, s^{-1}
2.5×10^{-3}	1.06×10^{-4}	8.0×10^{-3}	1.00×10^{-4}
4.0×10^{-3}	1.07×10^{-4}	9.5×10^{-3}	1.19×10^{-4}
6.0×10^{-3}	1.19×10^{-4}	1.25×10^{-2}	1.02×10^{-4}

$Mn^{III}Cl$, $[(Me_8TPP)Mn^{III}(ImH)]Cl$, and $[(Me_8TPP)Mn^{III}(ImH)_2]Cl$. The concentrations of these three species in any given reaction solution can be easily calculated from known initial concentrations of added reagents by use of eq 3 and 5. The relative distribution of these species at various concentrations of imidazole is shown in Figure 3.

An abbreviated scheme for oxygen transfer from NO to manganese(III) porphyrin species is provided in eq 8–11. In eq 8, NO forms a hydrogen-bonded complex with imidazole while eq 9–11 depict oxygen transfer from NO to $(Me_8TPP)Mn^{III}Cl$, $[(Me_8TPP)Mn^{III}(ImH)]Cl$, and $[(Me_8TPP)Mn^{III}(ImH)_2]Cl$, respectively. The reasonable assumption is made that only the

$$NO + ImH \overset{K_m}{\rightleftharpoons} NO\cdots HIm \quad (8)$$

$$(Me_8TPP)Mn^{III}Cl + NO \xrightarrow{k_1} [(Me_8TPP)(Cl)(MnO)] + DA \quad (9)$$

$$[(Me_8TPP)Mn^{III}(ImH)]Cl + NO \xrightarrow{k_2} [(Me_8TPP)(ImH)(MnO)]Cl + DA \quad (10)$$

$$[(Me_8TPP)Mn^{III}(ImH)_2]Cl + NO \xrightarrow{k_3} [(Me_8TPP)(ImH)_2(MnO)]Cl + DA \quad (11)$$

non-hydrogen-bonded NO (eq 8) is capable of transferring its oxygen. The assumption of the formation of an unreactive complex of NO and ImH (eq 8) is required in the computer fitting of the line which correlates the experimental points of Figure 2. A hydrogen-bonded complex of NO with ImH has been observed by use of ^1H NMR spectroscopy by Dr. Paul Nakagaki of this laboratory.[12] The equilibrium constants for hydrogen bonding of imidazole with *N,N*-dimethylacetamide, tri-*n*-butyl phosphate, and tri-*n*-octylphosphine oxide in $CHCl_3$ have been determined as 7.1, 86, and 230 M^{-1}, respectively.[13] These values may be compared to the equilibrium constant of 30 ± 10 M^{-1}, determined by computer fitting for imidazole hydrogen bonding to NO.

The value of k_{obsd}, at any concentration of ImH, is a weighted sum of contributions by the terms $k_1[(Me_8TPP)Mn^{III}Cl]$, $k_2[[(Me_8TPP)Mn^{III}(ImH)]Cl]$, and $k_3[(Me_8TPP)Mn^{III}(ImH)_2]Cl]$. Hence, taking into consideration that only unassociated NO reacts, the expression for k_{obsd} can be derived from eq 3 and 5 and 8–11. By use of eq 12, it is possible with the aid of a computer to

$$k_{obsd} = \left(\frac{1}{1 + K_m[ImH]}\right)\left(\frac{k_1 + k_2K_1[ImH] + k_3\beta_2[ImH]^2}{1 + K_1[ImH] + \beta_2[ImH]^2}\right) \quad (12)$$

determine the value of k_{obsd} for different ImH concentrations at a given concentration of catalyst. Such a computer-simulated line correlates the experimental points as shown in Figure 2. The constants required for the curve fitting are given in Table I. Constants k_1, K_1, and β_2 have been experimentally determined, while the remaining constants k_2, k_3, and K_m were obtained by nonlinear least-squares computer fitting of k_{obsd} to eq 12.[11] We note the large errors in the values for K_m and k_3. These two values are strongly correlated,[11] and that might be the source of large uncertainties. The error in k_3 is larger than the value of k_3 itself, indicating that k_3 might have a value of zero. This is not unreasonable, since k_3 is associated with coordinatively saturated Mn^{III} porphyrin with no available axial positions to participate in oxygen transfer.

Influence of varying imidazole concentration upon the product distribution was examined by HPLC analyses at 280 and 320 nm concurrent with the kinetic study. The concentrations of the six known products, DA, MA, A, FA, H, and MD, were determined at each $[ImH]_i$ (Table II). A 240-fold increase in $[ImH]_i$ gradually increases the amount of DA formed, from 44% at $[ImH]_i = 2.32 \times 10^{-4}$ M to 69% at $[ImH]_i \sim 5.64 \times 10^{-2}$ M. Formation of MA seems to be greatly affected by the concentration of imidazole. The percent of MA decreases rapidly from 33% at $[ImH]_i = 2.32 \times 10^{-4}$ M to its lowest of 5% at $[ImH]_i \sim 1.86 \times 10^{-3}$ M (close to rate maximum); thereafter, the percent of MA produced increases gradually to 39% ($[ImH]_i \sim 3.76 \times$

(12) From ^1H NMR studies in CD_2Cl_2 at constant ImH (0.01 M), variation of [NO] from 0.01 to 0.003 M caused an upfield shift (3.590 to 3.651 ppm) in the methyl peak (NMe_2) position of NO, indicating H bonding through the lone pairs of the oxygen. A similar change in the ratio ImH:NO ($[NO]_i$ decreases) caused a large change in the imidazole N–H peak position from 8.410 to 11.614 ppm, indicative of an increase in the H bonding of the imidazole. Imidazole, in general, exists in solution as highly organized H-bonded chains, and addition of NO actually disrupts these chains and hence caused the shift in N–H peak position.

(13) Wang, S.-M.; Lee, L.-Y.; Chen, J.-T. *Spectrochim. Acta* **1979**, *35*, 765.

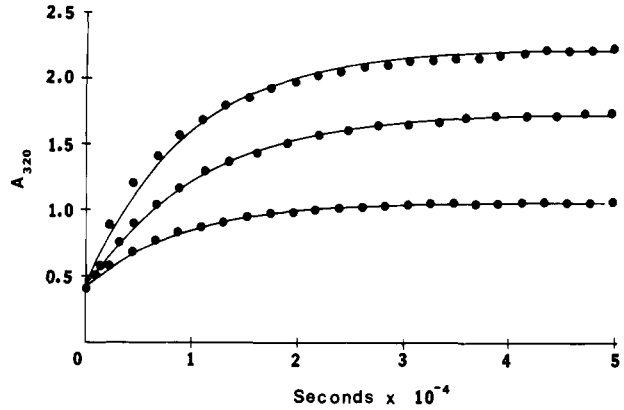

Figure 4. Plots of A_{320} vs. time for the reaction of $(Me_8TPP)Mn^{III}Cl$ (1.23×10^{-4} M) plus ImH (1.15×10^{-3} M) with varying concentrations of NO ($[NO]_i = 2.5 \times 10^{-3}$, 8.0×10^{-3}, and 1.25×10^{-2} M). Points are experimental, and the lines have been computer generated by use of the first-order rate law ($k_{obsd} = 1.06 \times 10^{-4}$, 1.00×10^{-4}, and 1.02×10^{-4} s^{-1}, respectively). The plots show that the initial rates are dependent on $[NO]_i$ but that the pseudo-first-order rate constants (k_{obsd}) are not.

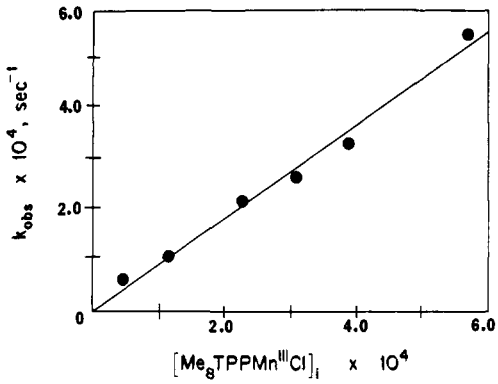

Figure 5. Plot of k_{obsd} vs. $[(Me_8TPP)Mn^{III}Cl]_i$ showing the linear dependence of k_{obsd} on $[(Me_8TPP)Mn^{III}Cl]_i$ ($[NO]_i = 1.49 \times 10^{-3}$ M and $[ImH]_i = 2.11 \times 10^{-3}$ M). The slope yields an apparent second-order rate constant of 0.92 M^{-1} s^{-1}.

10^{-2} M). There are no observable trends in respect to formation of A, FA, H, and MD, though traces, or complete absence of these products, are noted at $[ImH]_i = 0$ or when $[ImH]_i > 9.4 \times 10^{-3}$ M. The yield of formaldehyde based on the method of Nash[14] is reported in Table II.

Material balance between reactants and identifiable products is influenced by the initial concentration of imidazole (Table II). In the absence of ImH there is complete material balance between reactants and products in N and O. On addition of ImH there is loss of material balance in both N and O, this loss reaching a maximum at the maximum value of k_{obsd} where the concentration of the $[Me_8TPP)Mn^{III}(ImH)]Cl$ species is maximal. The variation in the concentrations of $(Me_8TPP)Mn^{III}Cl$, $[(Me_8TPP)Mn^{III}(ImH)]Cl$, and $[(Me_8TPP)Mn^{III}(ImH)_2]Cl$ with change in $[ImH]_i$ is shown in Figure 3. At $[ImH]_i \sim 1.16 \times 10^{-3}$ and 1.32×10^{-3} M there is an unaccountability for 27% of N in the products. The O imbalance increases from 14% at $[ImH]_i \sim 2.32 \times 10^{-4}$ M to a maximum loss of ~65% at $[ImH]_i \sim 1.32 \times 10^{-3}$ and 1.86×10^{-3} M. The lack of N material balance can be accounted for in the formation of several unidentified products appearing at retention times 7.36 (λ_{max} 289 nm), 19.04 (λ_{max} 275 nm), 24.45, 47.96 (λ_{max} 263 nm), and 53.06 min. A careful examination of product distribution at high [ImH] shows an increase in the yield of DA, with MA being the only oxidation product of DA. At the same time more oxygen originating in NO remains unaccounted for, suggesting that imidazole serves as an oxidizable substrate, which at high concentration prevents further oxidation of DA.

(14) Nash, T. *Biochem. J.* **1953**, *55*, 416.

Table IV. Effect of $[TBPH]_i$ on the Rate of Formation of TBP• (Monitored at 630 nm) and the Product Yields (Based on $[NO]_i = 2.95 \times 10^{-3}$ M) with $[(Me_8TPP)Mn^{III}Cl]_i = 1.06 \times 10^{-4}$ M and $[ImH]_i = 3.50 \times 10^{-3}$ M

	percentage yields			
$[TBPH]_i$, M	DA	MA	TBP•	k_{obsd}, s^{-1}
0	58	19	0	9.7×10^{-5}[a]
0.028	73	29	69	1.20×10^{-4}
0.069	75	26	75	1.06×10^{-4}
0.173	75	26	78	1.01×10^{-4}
0.277	68	29	65	1.07×10^{-4}

[a] Monitored at 320 nm.

Evidence for the oxidation of ImH by $[(TPP)(Cl)(ImH)(MnO)]^+$ has been previously shown when *tert*-BuOOH serves as the oxygen donor.[4b]

Dependence of k_{obsd} upon $[(Me_8TPP)Mn^{III}Cl]_i$ and $[NO]_i$ for the Reaction of NO with Manganese(III) Porphyrin in the Presence of ImH. At constant $[(Me_8TPP)Mn^{III}Cl]_i = 1.23 \times 10^{-4}$ M and $[ImH]_i = 1.15 \times 10^{-3}$ M, the pseudo-first-order rate constant, k_{obsd}, for the decomposition of NO does not vary, within experimental error, with change in $[NO]_i$ (Table III). This observation is consistent with the increase in initial rates on increase in $[NO]_i$ (Figure 4). The reaction is, therefore, first order in NO. The manganese(III) porphyrin concentration was varied in the range 5.7×10^{-5} to 5.49×10^{-4} M at constant $[ImH]_i$ (2.11×10^{-3} M) and $[NO]_i$ (1.49×10^{-3} M). The results are given in Figure 5. The pseudo-first-order rate constant, k_{obsd}, is a linear function of $[(Me_8TPP)Mn^{III}Cl]_i$. The reaction is, therefore, first order in manganese(III) porphyrin catalyst. The slope of Figure 5 provides an apparent second-order rate constant of 0.92 M^{-1} s^{-1} based upon total manganese(III) porphyrin concentration. At the $[ImH]_i$ employed, the mole percentage of $[(Me_8TPP)Mn^{III}Cl]$ to $[[(Me_8TPP)Mn^{III}(ImH)]Cl]$ to $[[(Me_8TPP)Mn^{III}(ImH)_2]Cl]$ = 44:22:34.

Reaction in the Presence of 2,4,6-Tri-*tert*-butylphenol (TBPH). Oxidation of 2,4,6-tri-*tert*-butylphenol (TBPH) was monitored at the λ_{max} of the phenoxyl radical product (TBP•) at 630 nm (ϵ_{630} = 400 M^{-1} cm^{-1}). Experiments were carried out with the following *initial concentrations of the other reactants*: $[NO]_i = 2.95 \times 10^{-3}$ M, $[ImH]_i = 3.50 \times 10^{-3}$ M, and $[(Me_8TPP)Mn^{III}Cl]_i = 1.06 \times 10^{-4}$ M. The percentage yields of DA, MA, and TBP• products at completion of the reaction are provided in Table IV. Examination of Table IV shows that the pseudo-first-order rate constants for TBP• formation, at varying $[TBPH]_i$, remained reasonably constant with an average value, $k_{obsd} = 1.09 \times 10^{-4}$ s^{-1}, and shows the oxygen transfer N → Mn is rate determining. This compares well with the value of k_{obsd} determined in the absence of TBPH by monitoring DA appearance at 320 nm, $k_{obsd} = 9.7 \times 10^{-5}$ s^{-1}. Based upon the $[NO]_i$ used, TBPH traps, by average, approximately 72% of the higher valent manganese–oxo porphyrin species at all concentrations of TBPH employed. This observation is consistent with the formation of ~73% DA and ~28% MA when $[TBPH]_i$ is between 0.028 and 0.277 M. No other N-containing products are formed.

Time Course for the Formation of each Reaction Product in the Decomposition of NO (3.03×10^{-3} M) when $[(Me_8TPP)Mn^{III}Cl] = 1.11 \times 10^{-4}$ M and $[ImH]_i = 3.60 \times 10^{-3}$ M. Reactions were carried out under nitrogen, and aliquots were withdrawn under flowing N_2 into gas-tight nitrogen-filled vials with immediate quenching into liquid nitrogen and later stored over dry ice until analyzed. Plots of concentration vs. time for the products DA, MA, H, and MD (determined by HPLC analysis) are shown in Figure 6A–D. For the production of DA and MA (Figure 6A and 6B) the plots fitted to the experimental points represent best fits to the first-order rate law for at least $7 \times t_{1/2}$. The first-order rate constants for the formation of DA and MA (8.1×10^{-5} and 7.3×10^{-5} s^{-1}, respectively) are in good agreement with the spectrally determined (320 nm) first-order rate constant for the appearance of DA plus MA (1.13×10^{-4} s^{-1}) when one considers the scattering in points for the HPLC method. Examination of Figure 6C and 6D shows lag phases in the formation of H and

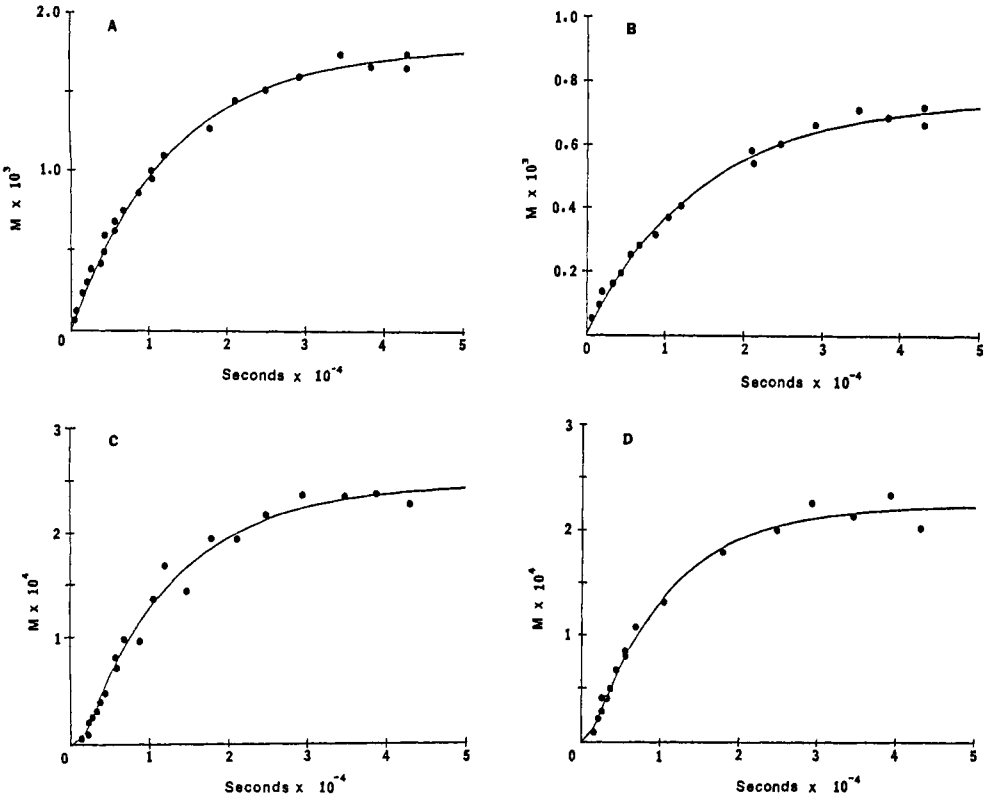

Figure 6. Plot of the time courses (determined by HPLC) for the products that are formed in the decomposition of $[NO]_i$ (3.03×10^{-3} M) in the presence of $(Me_8TPP)Mn^{III}Cl$ (1.11×10^{-4} M) and ImH (3.60×10^{-3} M): (A) *p*-cyano-*N*,*N*-dimethylaniline; (B) *p*-cyano-*N*-methylaniline; (C) *N*,*N*'-dimethyl-*N*,*N*'-bis(*p*-cyanophenyl)hydrazine; and (D) *N*,*N*'-bis(*p*-cyanophenyl)-*N*-methylmethylenediamine.

Table V. Effect of [Alkene] on the Product Yields and k_{obsd} for the Reaction of NO (2.9×10^{-3} M) with $(Me_8TPP)Mn^{III}Cl$ at constant $[ImH]_i$ (3.50×10^{-3} M)

[alkene]$_i$, M	[$(Me_8TPP)Mn^{III}Cl$]$_i$, M	percentage yields							k_{obsd}, s^{-1}
		DA	MA	H	FA	A	MD	epoxide	
0	1.22×10^{-4}	58	17	8	1	2	8		1.01×10^{-4}
TME									
0.01	1.13×10^{-4}	61	21	6	0	0	5	11	1.16×10^{-4}
0.10		72	22	3	0	0	3	49	1.09×10^{-4}
1.00		79	24	1	0	0	0	82	9.04×10^{-5}
cis-cyclooctene									
0.01	1.13×10^{-4}	62	18	7	0	0	5	29	1.18×10^{-4}
0.10		75	22	2	0	0	1	69	1.04×10^{-4}
1.00		79	21	0	0	0	0	81	9.30×10^{-5}
1.38	1.23×10^{-4}	83	20	0	0	0	0	82	
cyclohexene									
0.01	1.22×10^{-4}	68	21	7	2	1	9	23	9.80×10^{-5}
0.10		76	22	2	trace	2	3	46	1.07×10^{-4}
1.00		82	21	0	0	0	0	81	1.05×10^{-4}
norbornylene									
1.00	1.23×10^{-4}	82	20	0	0	0	0	82	
cyclopentene									
0.50	1.13×10^{-4}	75	19	0	0	0	0	51	
1.00		79	20	0	0	0	0	80	
trans-β-methylstyrene									
0.50	1.13×10^{-4}	68	19	3	0	trace	3	11	
1.00		72	20	1	0	0	1	11	

MD. Products A and FA were found in approximately 1% each after $7 \times t_{1/2}$.

Epoxidation of Alkenes in the Presence of Imidazole ($\sim 3.5 \times 10^{-3}$ M), $(Me_8TPP)Mn^{III}Cl$ (1.13×10^{-4} to 1.23×10^{-4} M), and NO (2.9×10^{-3} M). Table V summarizes the product yields for the reactions investigated and includes the pseudo-first-order rate constants (monitored at 320 nm) for a number of reactions. At high $[alkene]_i$ = 1.0 M all of the alkenes, except *trans*-β-methylstyrene (11%), yielded epoxide at ~80% based upon $[NO]_i$. (The low yield with *trans*-β-methylstyrene is consistent with the finding of others using PhIO, etc. with manganese porphyrin.[5c]) In all instances at [alkene] = 1.0 M, the yield of DA (from HPLC analysis) corresponds reasonably well with the yield of epoxide (from GC analysis). As evidenced from the results in Table V, the yields of DA and epoxide increase and the yields of demethylation products decrease with increase in alkene concentrations. At high $[alkene]_i$, epoxidation is favored over oxidation of DA and further oxidation of MA, hence, decreasing the yield of A, FA, H, and MD. The presence of alkene up to 1.0 M has virtually no effect on k_{obsd}.

Epoxidation of *cis*-cyclooctene (1.38 M) at constant $(Me_8TPP)Mn^{III}Cl$ (1.23×10^{-4} M) and NO (2.89×10^{-3} M) with varying imidazole concentrations was investigated. In the absence of imidazole no epoxide was detected (GC), and the HPLC

analysis yields DA (19%), MA (71%), H (trace), 2% of 4-cyano-7-(dimethylamino)-2-benzofuranone-3-spiro-2′-cyano-5′-(dimethylamino)cyclopentadiene,[15] and several other products which have not been identified. Upon addition of imidazole, the epoxide formed with maximum yield (~87% at $[ImH]_i = 1.17 \times 10^{-3}$ M) (Table VI). Further increase in $[ImH]_i$ resulted in a drop of epoxide yield to ~65% at $[ImH]_i = 3.76 \times 10^{-2}$ M.

Discussion

In this investigation there is examined the effect of imidazole as a ligand in the reaction of *p*-cyano-*N*,*N*-dimethylaniline *N*-oxide (NO) with (*meso*-tetrakis(2,6-dimethylphenyl)porphinato)manganese(III) chloride ($(Me_8TPP)Mn^{III}Cl$) in dry CH_2Cl_2 (25 ± 0.2 °C) under anaerobic conditions. In a previous study it was shown that exchange of Cl^- ligand for imidazole (ImH) dramatically increases the second-order rate constants for the transfer of an oxygen from both percarboxylic acids and alkyl hydroperoxides to (tetraphenylporphinato)manganese(III).[4a] The present study establishes that such imidazole ligation also increases the rate constant for oxygen atom transfer from NO to the (*meso*-tetrakis(2,6-dimethylphenyl)porphinato)manganese(III) moiety. In addition, the specificity, as oxidants, of the various ligated higher valent manganese–oxo porphyrins has been examined.

Commitment Step. The formation of the major products of reaction of NO with $(Me_8TPP)Mn^{III}Cl$ in the absence and presence of varying concentrations of ImH follows the first-order rate law under the pseudo-first-order conditions of $[NO]_i \gg [(Me_8TPP)Mn^{III}Cl]_i$. The pseudo-first-order rate constants is found to be independent of $[NO]_i$ and linearly dependent upon $[(Me_8TPP)Mn^{III}Cl]_i$. All reactions, therefore, exhibit a first-order dependence upon both $[NO]_i$ and $[(Me_8TPP)Mn^{III}Cl]_i$.

That the rate-determining step involves oxygen transfer from NO to manganese(III) porphyrin species is clearly documented by several pertinent observations (among others) made in the following experiments. First, when employing 2,4,6-tri-*tert*-butylphenol (TBPH) as a $1e^-$ oxidizable substrate, it is found that the pseudo-first-order rate constant for TBP• formation is independent of $[TBPH]_i$ (0.028–0.277 M; Table IV). The second-order rate constant, calculated from the average value of k_{obsd} for these experiments ($k_{obsd}/[(Me_8TPP)Mn^{III}Cl]_i = 1.02\ M^{-1}\ s^{-1}$), is comparable ($0.92\ M^{-1}\ s^{-1}$) to that for the formation of DA and MA products in the absence of TBPH. Thus, TBPH oxidation to TBP• is not rate controlling, and the commitment step must be oxygen transfer from NO to manganese(III) porphyrin species. Second, the rates of epoxidation of 2,3-dimethyl-2-butene (TME), *cis*-cyclooctene, and cyclohexene are independent of the concentration of the respective alkene (0.01–1.0 M). Thus, with the same initial concentrations of ImH and $(Me_8TPP)Mn^{III}Cl$ for epoxidation of TME, *cis*-cyclooctene, and cyclohexene, the average values of k_{obsd} are 1.05×10^{-4}, 1.05×10^{-4}, and $1.03 \times 10^{-4}\ s^{-1}$, respectively. In the absence of alkene, the value of k_{obsd} for the formation of DA and MA is $1.01 \times 10^{-4}\ s^{-1}$. Thus, different alkenes are epoxidized with the same rate constant. Alkene epoxidation is not rate controlling, and the commitment step is again oxygen transfer from NO to manganese(III) porphyrin species. This last observation is in contradistinction with the results of Collman and co-workers,[5a] who used hypochlorite as the oxygen-transfer agent and a solvent biphase of H_2O/toluene with phase-transfer catalyst. Their results support alkene dependency in the rate-limiting step, and they have postulated the formation of a metallaoxetane intermediate whose breakdown is the rate-determining step of the catalytic cycle. If such an intermediate were to be formed in the present system, it would arise after the rate-limiting transfer of oxygen to manganese(III) porphyrin. Our observations do not contradict those from Collman's laboratory. Oxygen transfer from hypochlorite is likely to be much more facile than is oxygen transfer from NO, because Cl^- is a better leaving group than is *p*-cyano-*N*,*N*-dimethylaniline (DA) and, of course, the solvent systems employed are quite different (eq 13).

Table VI. Effect of $[ImH]_i$ on the Product Yields in the Epoxidation of *cis*-Cyclooctene (1.38 M) with $[(Me_8TPP)Mn^{III}Cl]_i = 1.23 \times 10^{-4}$ M and $[NO]_i = 2.89 \times 10^{-3}$ M

	percentage yields		
$[ImH]_i$, M	DA	MA	epoxide
0	19	71	0
4.70×10^{-4}	83	17	83
1.17×10^{-3}	85	18	87
1.86×10^{-3}	86	19	84
3.38×10^{-3}	83	20	82
4.14×10^{-3}	80	20	79
9.40×10^{-3}	81	19	65
3.76×10^{-2}	80	20	65

$$(Porph)(ImH)Mn^{III}OCl \rightarrow [(Porph)(ImH)(MnO)]^+ + Cl^-$$

$$(Porph)(ImH)Mn^{III}ON \rightarrow [(Porph)(ImH)(MnO)]^+ + DA \quad (13)$$

Influence of ImH Concentration on Rates and Products. In distinction to the finding that the rate of oxygen transfer from percarboxylic acids and alkyl hydroperoxides continually increases with increase in imidazole concentration[4a] when using (tetraphenylporphinato)manganese(III) chloride ($(TPP)Mn^{III}Cl$), we now observed that the rate of oxygen transfer from NO, using $(Me_8TPP)Mn^{III}Cl$, first increases to a maximum at $[ImH] = 2.4 \times 10^{-3}$ M and then decreases. The experimental data may be explained by consideration of the equilibrium and reactions of eq 8–11. This is shown in the plot of k_{obsd} vs. $[ImH]_i$ of Figure 2. The points represent experimental data, and the line has been computer generated from eq 12 by using the constants of Table I. From equilibrium constants (K_1 and β_2), the concentrations of the species $(Me_8TPP)Mn^{III}Cl$, $[(Me_8TPP)Mn^{III}(ImH)]Cl$, and $[(Me_8TPP)Mn^{III}(ImH)_2]Cl$ may be calculated as a function of $[ImH]_i$ at any given concentration of total manganese(III) porphyrin (Figure 3). The ratios of the second-order rate constants for the reaction of the $(Me_8TPP)Mn^{III}Cl$, $[(Me_8TPP)Mn^{III}(ImH)]Cl$, and $[(Me_8TPP)Mn^{III}(ImH)_2]Cl$ species with NO may be calculated to be 1.0:166 ± 18:2.2 ± 2.7. Over the range of imidazole concentrations employed k_{obsd} is dominated by k_2-$[(Me_8TPP)Mn^{III}(ImH)]Cl$. Catalysis of epoxidation by $[(Me_8TPP)Mn^{III}(ImH)_2]Cl$ may or may not be of significance. Because bis-axial ligation by ImH in the species $[(Me_8TPP)Mn^{III}(ImH)_2]Cl$ prevents approach of NO to the manganese(III) moiety, it is most obvious that this species should not react with NO. Any reactivity by this species must be due to the participation of a structural isomer in unfavorable equilibrium with $[(Me_8TPP)Mn^{III}(ImH)_2]Cl$. This minor component would likely represent $[(Me_8TPP)Mn^{III}(ImH\cdots ImH)]Cl$ (eq 14). Imidazoles

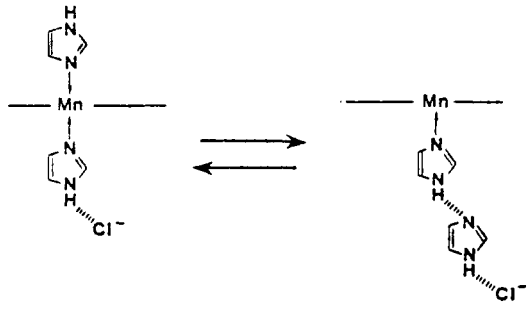

$[(Me_8TPP)Mn^{III}(ImH)_2]Cl$ $[(Me_8TPP)Mn^{III}(ImH\cdots ImH)]Cl$ (14)

are known to exist in H-bonded chains in aprotic solvents,[11] and the type of ligation proposed for $[(Me_8TPP)Mn^{III}(ImH\cdots ImH)]Cl$ has previously been considered by Valentine.[16] The endergonicity

(15) Ostovic, D.; Knobler, C. B.; Bruice, T. C. *J. Am. Chem. Soc.*, third paper in a series in this issue.

(16) Quinn, R.; Nappa, M.; Valentine, J. S. *J. Am. Chem. Soc.* **1982**, *104*, 2588.

of the equilibrium of eq 14 is undoubtedly such that any second-order rate constant calculated for the reaction of NO with $[(Me_8TPP)Mn^{III}(ImH)_2]Cl$ is much smaller than the true rate constant for $[(Me_8TPP)Mn^{III}(ImH\cdots ImH)]Cl$. The species $[(TPP)Mn^{III}(ImH\cdots ImH)]Cl$ has been found to be an important reactive component when percarboxylic acids and alkyl hydroperoxides serve as oxygen-transfer agents.[4a]

p-Cyano-*N*,*N*-dimethylaniline *N*-oxide serves as a dual reagent in its reaction with metal(III) porphyrin salts insofar that it carries out a $2e^-$ oxidation of the metal(III) porphyrin, transfers an oxygen to the metal atom, and also supplies DA as an oxidizable substrate. The species $(Me_8TPP)Mn^{III}Cl$, $[(Me_8TPP)Mn^{III}(ImH)]Cl$, and possibly $[(Me_8TPP)Mn^{III}(ImH\cdots ImH)]Cl$ react with NO to provide higher valent manganese oxo species which possess different reactivities and specificities (see Table II).

The time course for the formation of each product in the reaction of NO with $(Me_8TPP)Mn^{III}Cl$ has been determined at $[ImH]_i = 3.60 \times 10^{-3}$ M. At this concentration of ImH, the mole percentages of total manganese(III) porphyrin are as follows: $(Me_8TPP)Mn^{III}Cl$, 24.8%; $[(Me_8TPP)Mn^{III}(ImH)]Cl$, 21%; and $[(Me_8TPP)Mn^{III}(ImH)_2]Cl$, 54.1%. The principal reactant is $[(Me_8TPP)Mn^{III}(ImH)]Cl$, being more reactive than the other two. The formation of both DA and MA (by HPLC analysis) follows the first-order rate law (Figure 6A and 6B) with rates constants comparable to that determined spectrophotometrically for the sum of products formation. Finding the rate of formation of DA and its oxidation product MA to be equivalent supports $N \rightarrow Mn$ oxygen transfer as rate determining. The appearance of H and MD are associated with lag phases followed by their first-order buildup. The observation of lag phases in the formation of H and MD is not unexpected, as these products form by coupling of MA$^\bullet$ species, and they arise by way of a sequence of reactions (DA $\rightarrow$ MA $\rightarrow$ MA$^\bullet$; 2MA$^\bullet \rightarrow$ H, 2MA$^\bullet \rightarrow$ MD) which follow the rate-determining oxygen transfer from NO.

The influence of the concentration of imidazole on the yields of DA and MA is provided in Figure 7. With increase in $[ImH]_i$ the concentration of DA increases and then becomes constant above $[ImH] = 1 \times 10^{-2}$ M. The mole percent of a particular manganese(III) porphyrin species, present when multiplied by the relative second-order rate constant for its reaction with NO, provides a number which is proportional to the fraction of NO which reacts with said catalytic species. The increase in DA follows the continual decrease in $(Me_8TPP)Mn^{III}Cl$, and formation of DA becomes constant when the reaction of NO occurs with $[(Me_8TPP)Mn^{III}(ImH)]Cl$ and $[(Me_8TPP)Mn^{III}(ImH)_2]Cl$. Thus, the higher valent manganese–oxo porphyrin species generated from $(Me_8TPP)Mn^{III}Cl$ is the best oxidizing agent for DA. On increase of ImH, formation of MA first decreases until the concentration of $[(Me_8TPP)Mn^{III}(ImH)]Cl$ reaches a maximum (at 22 mol % of total manganese porphyrin) and then increases. The increase in the yield of MA levels off at ~40%, where $[(Me_8TPP)Mn^{III}Cl]$ is insignificant, and the mole percent of $[(Me_8TPP)Mn^{III}(ImH)]Cl$ decreases from 12% to ~2.4% while the mole percent of $[(Me_8TPP)Mn^{III}(ImH)_2]Cl$ varies from 83% to 97.5%. Formation of MA from DA is accompanied by the formation of formaldehyde (eq 15). Inspection of Table II shows

$$DA \xrightarrow{\text{"oxene" equivalent}} MA + CH_2O \qquad (15)$$

that the percent yield of CH_2O is constant (±5%) with change in the concentration of imidazole. This suggests that the minimum in yield of MA is due to its oxidation. The decrease in MA yield occurs as the manganese–oxo species formed from $[(Me_8TPP)Mn^{III}(ImH)]Cl$ reaches a maximum concentration, and the gain in MA yield with further increase in $[ImH]_i$ suggests that the manganese–oxo porphyrin species formed from $[(Me_8TPP)Mn^{III}(ImH)]Cl$ is most adept at MA oxidation. From Table II, the yields of identified products of MA oxidation do not increase as MA yield decreases. Also, the decrease in MA yield is associated with a N imbalance between the reactant (NO) and products. From these observations it is concluded that the decrease in MA concentration is due to its oxidative combination (as MA$^\bullet$) with imidazole, etc., to provide a number of detected (see Results)

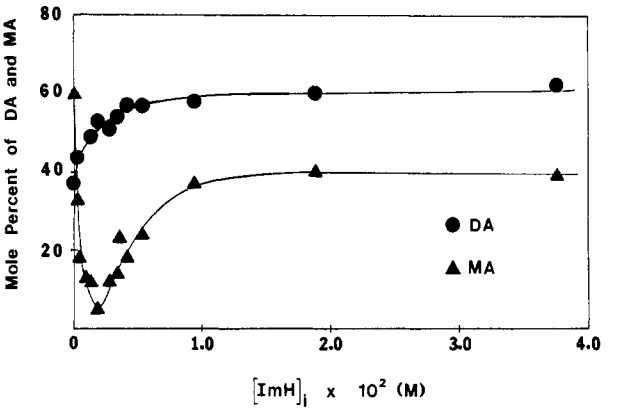

Figure 7. Plot of percentage yields of DA (●) and MA (▲) for the reaction of $[NO]_i = 2.87 \times 10^{-3}$ M with $[(Me_8TPP)Mn^{III}Cl]_i = 1.22 \times 10^{-4}$ M at varying $[ImH]_i$. The percentage yields are based upon the initial concentration of NO.

but unidentified products. It should be noted that the products H and MD are formed by combinations of MA$^\bullet$ species. At the highest concentrations of ImH, DA (69%) and MA (32%) are the only oxidation products, and there is complete material balance in nitrogen between NO and these products.

Epoxidation of Alkenes. Results for the epoxidation of a series of alkenes under fixed reactant conditions such that $[(Me_8TPP)Mn^{III}Cl]:[[(Me_8TPP)Mn^{III}(ImH)]Cl]:[[(Me_8TPP)Mn^{III}(ImH)_2]Cl] = 25:21:54$ are provided in Table V. The influence of changing the concentration of ImH upon the epoxidation of *cis*-cyclooctene at constant initial concentrations of $(Me_8TPP)Mn^{III}Cl$ is provided in Table VI. The lack of epoxidation of *cis*-cyclooctene by NO plus $(Me_8TPP)Mn^{III}Cl$ in the absence of ImH as compared to the high yield (80%) of cyclooctene epoxide obtained with $(Me_8TPP)Fe^{III}Cl$ + NO clearly illustrates[2e] that the $[(Me_8TPP)(Cl)(MnO)]^+$ species, though the better $1e^-$ oxidant, possesses no appreciable ability to carry out an "oxene" equivalent transfer reaction. Clearly, manganese porphyrin, $2e^-$ oxidized above the porphyrin manganese(III) state, has at least two different electronic structures whose presence is dictated by the nature of an axial ligand. The nature of the structures awaits further exploration. The maximum yield of epoxide is obtained in the range of [ImH] where $[(Me_8TPP)Mn^{III}(ImH)(Cl)]$ is maximal. It follows that the most important epoxidizing agent is formed from reaction of NO with $[(Me_8TPP)Mn^{III}(ImH)]Cl$.

The yields of DA and MA remain relatively constant with change in $[ImH]_i$ in the presence of *cis*-cyclooctene. The yield of *cis*-cyclooctene oxide is seen to equal the yield of DA except for the highest concentrations of ImH when the yield of epoxide decrease but the yield of DA remains constant. This suggests that unidentified products are formed from the alkene at the highest ImH concentrations. Material balance is obtained in all epoxidation reactions insofar that the knonw products account for all N and O of the *N*-oxide. Any conjugated product formed from the alkene would, therefore, arise by combination of ImH and alkene-derived species.

Oxidations within a Solvent Cage. 2,4,6-Tri-*tert*-butylphenol (TBPH) served well as a trap for the $(^{+\bullet}TPP)Fe^{IV}O$ species generated from $(TPP)Fe^{III}Cl$ with NO.[2c] This was shown from the observation that formation of both DA and the TBPH oxidation product, TBP$^\bullet$, was quantitative. However, TBPH was found to trap only 72% of the higher valent manganese–oxo porphyrin species in the reaction of NO with $(Me_8TPP)Mn^{III}Cl$ in the presence of imidazole. Aside from TBP$^\bullet$ (72%), the only other products are DA (73%) and MA (28%). The yields of TBP$^\bullet$, DA, and MA provide material balance in both N and O. At the concentration of ImH employed there was present 26% $(Me_8TPP)Mn^{III}Cl$, 21% $[(Me_8TPP)Mn^{III}(ImH)]Cl$, and 53% $[(Me_8TPP)Mn^{III}(ImH)_2]Cl$. The inability to quantitatively trap the higher valent manganese–oxo porphyrin species does not necessarily mean that TBPH is an inefficient trap. This maximum

yield of epoxide is dependent upon $[ImH]_i$ (Table VI), but in all cases alkene does not trap all higher valent manganese–oxo species. Examination of Table V shows that at 1.0 M in 2,3-dimethyl-2-butene, *cis*-cyclooctene, cyclohexene, norbornylene, or cyclopentene there is obtained ~80% yields of the corresponding epoxides. The results with TBPH and alkenes suggest the possibility that a portion of DA oxidation occurs within a solvent cage, as previously found for the reaction of $(TPP)Mn^{III}X$ ($X^- = F^-$, Cl^-, Br^-, OCN^-) with NO (see eq 1).[1] Any other explanation based upon a preference for either $1e^-$ oxidation or epoxidation by the imidazole-ligated higher valent manganese–oxo porphyrin species may be discounted, because neither the $1e^-$ oxidizable TBPH nor alkenes are capable of completely trapping the oxo species.

Acknowledgment. This work was supported by a grant from the American Cancer Society and the National Institutes of Health. W.-H.W. expresses appreciation to the Universiti Malaya, Kuala Lumpur, Malaysia, for a sabbatical leave of absence during the tenure of this study. We should like to express appreciation to a referee for helpful comments.

Kinetics and Mechanism of Oxygen Transfer in the Reaction of *p*-Cyano-*N*,*N*-dimethylaniline *N*-Oxide with Metalloporphyrin Salts. 6.[1,2] Oxygen Atom Transfer to and from the Iron(III) C_2cap Porphyrin of Baldwin

Thomas C. Bruice,* C. Michael Dicken, P. N. Balasubramanian, T. C. Woon, and Fu-Lung Lu

Contribution from the Department of Chemistry, University of California at Santa Barbara, Santa Barbara, California 93106. *Received September 19, 1986*

Abstract: The decomposition of *p*-cyano-*N*,*N*-dimethylaniline *N*-oxide (NO) is catalyzed (CH_2Cl_2 solvent at 25 °C) by the SbF_6^- salt of the C_2-capped (*meso*-tetraphenylporphinato)iron(III) of Baldwin ($(TPPC_2cap)Fe^{III}SbF_6$). Since neither NO nor the SbF_6^- anion can fit under the cap, this result establishes that oxygen transfer from NO to the iron(III) center can occur without the intermediate iron(IV)–oxo porphyrin π-cation being hexacoordinated. The products of NO decomposition (*p*-cyano-*N*,*N*-dimethylaniline (DA) 68%, *p*-cyano-*N*-methylaniline (MA) 12%, *p*-cyanoaniline (A) 1%, *N*-formyl-*p*-cyano-*N*-methylaniline (FA) 6%, *N*,*N*'-dimethyl-*N*,*N*'-bis(*p*-cyanophenyl)hydrazine (H) 7%, and CH_2O 3%) account for 100% of the *p*-cyanodimethylaniline moiety of NO, but ca. 40% of the oxide oxygen of NO remains unaccounted for by product isolation. This is due to some loss of the catalyst and oxidation of the CH_2Cl_2 solvent during turnover. Oxidation of solvent results in the gradual exchange of the SbF_6^- axial ligand for Cl^-. Product formation on reaction of NO with $(TPPC_2cap)Fe^{III}SbF_6$ can be approximated by the first-order rate law. Since the observed first-order rate constants at a given $[NO]_i$ are a linear function of the iron(III) porphyrin, the reaction is first order in this catalyst and essentially so in NO. However, the finding that the initial rates are independent of $[NO]_i$ establishes that the iron(III) porphyrin catalyst is saturated with NO on initiation of the reaction. The exchange of Cl^- for SbF_6^- axial ligand and some loss of catalyst during turnovers are responsible for the reactions changing from initial zero order to essentially first order in $[NO]_i$. Trapping of the intermediate ($(^{+\bullet}TPPC_2cap)Fe^{IV}O$) by 2,4,6-tri-*tert*-butylphenol (TBPH), 2,3-dimethyl-2-butene (TME), and *p*-cyano-*N*-methylaniline (MA) prevents solvent oxidation and porphyrin oxidative destruction. Under these trapping conditions the reaction is rapid and zero order in NO to completion. That the zero-order kinetics are due to saturation of the $[(TPPC_2cap)Fe^{III}]^+$ catalysts by NO was established by following the time course of the reaction in the Soret and Q spectral regions. The products with TME are TME epoxide (100%) and DA (100%) while with TBPH the radical TBP$^\bullet$ (100%) and DA (100%) are formed. The rate is also increased, but to a lesser extent, when using the poorer substrates, cyclohexene and norbornylene. These substrates also impart a zero-orderness to the appearance of products. The kinetics for the reaction of $(TPPC_2cap)Fe^{III}SbF_6$ with NO using TME, TBPH, and MA as substrates have been computer simulated with the requirement of steady-state saturation in the intermediate $(TPPC_2cap)Fe^{III}ON$. For successful simulations it is required that both the formation of $(^{+\bullet}TPPC_2cap)Fe^{IV}O$ + DA from $(TPPC_2cap)Fe^{III}ON$ and the reaction of $(^{+\bullet}TPPC_2cap)Fe^{IV}O$ with substrates (i.e., TME, TBPH, and MA) are partially rate limiting. At concentrations of added alkene less than that required for trapping of $(^{+\bullet}TPPC_2cap)Fe^{IV}O$ there are obtained, by cycloaddition of DA$^\bullet$ radical and alkene, tetrahydroquinoline derivatives.

In previous papers we have described kinetic and mechanistic studies dealing with the use of *p*-cyano-*N*,*N*-dimethylaniline *N*-oxide (NO) as an oxygen-transfer agent to a number of iron(III),[1] manganese(III),[2] and chromium(III)[3] porphyrins in the oxidation of N,N-disubstituted and N-monosubstituted anilines, 1-phenyl-1,2-ethanediol, and a variety of electron-acceptor traps as well as the epoxidation of a variety of alkenes. The reaction of NO with (*meso*-tetraphenylporphinato)iron(III) chloride[1c] ($(TPP)Fe^{III}Cl$), (*meso*-tetra(2,6-dichlorophenyl)porphinato)iron(III) chloride[1d] ($(Cl_8TPP)Fe^{III}Cl$), and (*meso*-tetra(2,6-dimethylphenyl)porphinato)iron(III) chloride[1e] ($(Me_8TPP)Fe^{III}Cl$) involves rate-determining transfer of oxygen from N → Fe as shown by the trapping of the $(^{+\bullet}Porph)Fe^{IV}O$ species. The product of the trapping experiments, aside from oxidized trap, is *p*-cyano-*N*,*N*-dimethylaniline (DA). Because the formation of $(^{+\bullet}Porph)Fe^{IV}O$ species is rate determining, its structure cannot be determined by use of NO as the oxygen-transfer agent.

(1) (a) Shannon, P.; Bruice, T. C. *J. Am. Chem. Soc.* **1981**, *103*, 4500. (b) Nee, M. W.; Bruice, T. C. *Ibid.* **1982**, *104*, 6123. (c) Dicken, C. M.; Lu, F.-L.; Nee, M. W.; Bruice, T. C. *Ibid.* **1985**, *107*, 5776. (d) Dicken, C. M.; Woon, T.-C.; Bruice, T. C. *Ibid.* **1986**, *108*, 1636. (e) Woon, T.-C.; Dicken, C. M.; Bruice, T. C. *J. Am. Chem. Soc.* **1986**, *108*, 7990.

(2) Powell, M. F.; Pai, E. F.; Bruice, T. C. *J. Am. Chem. Soc.* **1984**, *106*, 3277.

(3) (a) Yuan, L.-C.; Bruice, T. C. *J. Am. Chem. Soc.* **1985**, *107*, 512. (b) Yuan, L.-C.; Calderwood, T. S.; Bruice, T. C. *Ibid.* **1985**, *107*, 8273.

0002-7863/87/1509-3436$01.50/0